Flow induced Grandjean lines in cholesteric liquid crystals

M. J. Press, A.S. Arrott

Classification
Physics Abstracts
61.30

FLOW INDUCED GRANDJEAN LINES IN CHOLESTERIC LIQUID CRYSTALS

M. J. PRESS and A. S. ARROTT

Department of Physics, Simon Fraser University, Burnaby, B.C. Canada V5A 1S6

(*Reçu le 5 janvier 1978, accepté le 29 mars 1978*)

Résumé. — Des lignes singulières régulièrement espacées apparaissent quand un cristal liquide cholestérique s'écoule entre deux lames de verre non parallèles puis restent en place quand l'écoulement a cessé. Les lames de verre sont traitées pour assurer un ancrage homéotrope à leurs surfaces, mais l'écoulement crée une région d'ancrage homogène faible proche des surfaces simulant ainsi les conditions pour le développement de lignes de Grandjean dans un coin de Cano. La relaxation vers une configuration cholestérique périodique produit des régions alternées distinguables par les *connectivités parallèles et antiparallèles* des champs de directeurs entre les deux surfaces. Les résultats d'un modèle à une constante élastique sont en accord qualitatif avec ceux d'une expérience faite avec une solution à 3 % d'oléate de cholestéryl dans du méthoxybenzylidènebutylaniline.

Abstract. — Regularly spaced singular lines appear when a cholesteric liquid crystal flows between glass plates inclined at a small wedge angle and remain after the flow ceases. The glass plates are treated to give homeotropic pinning at the surfaces, but the flow effectively creates a region of soft homogeneous pinning slightly away from the surfaces, thus simulating the conditions for development of Grandjean lines in a Cano wedge. Relaxation to the periodic cholesteric configuration produces alternating regions distinguished by parallel and antiparallel connectivity of the director fields between the two surfaces. Computations for a one constant elasticity model give qualitative agreement with experiment on a 3 % solution of cholesteryl oleate in methoxybenzylidene-butylaniline.

1. **Introduction.** — In a recent series of papers [1, 2] we described the periodic finger-like structures that are produced when a cholesteric liquid crystal is placed between approximately parallel glass plates which have been treated to give homeotropic alignment of the director field at their surfaces. In addition to these finger structures, referred to as PC for periodic cholesteric configurations, many other features are observed. One of these is the presence of singular lines which form in profusion when the sample is cooled down from the isotropic into the cholesteric phase, or when a large shearing pulse is sent through the sample, such as by tapping the constraining glass plates. A sample in the process of recovering from a large flow is shown in figure 1. By careful manipulation of these plates, most of these singular lines can be removed through the ensuing flow. The result of the controlled flow is to eliminate many of the regions which have randomly nucleated with one or the other of two principle configurations which are separated by the lines. We have termed these the 0-0 and 0-π configurations depending on whether the top and bottom surfaces of the sample are connected by a molecular structure which can be distorted continuously to the homeotropic (0-0) such as with the application of a vertical magnetic field as shown in figure 2, or cannot be driven to the homeotropic continuously with a vertical magnetic field (0-π) as shown in figure 3. These configurations can be distinguished optically in a magnetic field since between crossed polarizers the field of view of figure 2*b* observed in parallel light remains dark as the sample is rotated

FIG. 1. — A 3 % solution of cholesteryl oleate in methoxy-benzylidene-butylanaline observed between crossed polarizers with white light. The sample is flowing and many singular lines can be seen.

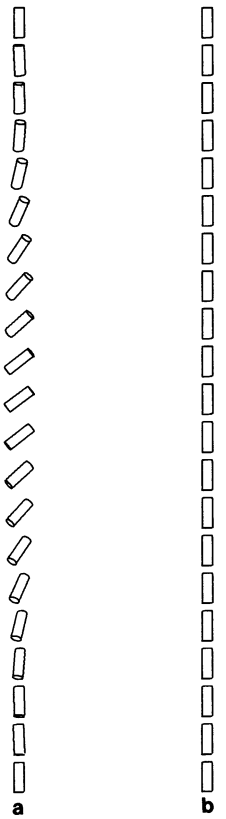

FIG. 2. — A possible molecular structure for a cholesteric in the 0-0 configuration subject to homeotropic pinning at the top and bottom surfaces. In (*a*) there is no applied magnetic field and a partially formed cholesteric helix is seen. In (*b*) a strong magnetic field has been applied perpendicular to the top and bottom surfaces. The cholesteric helix is destroyed and a homeotropic configuration produced.

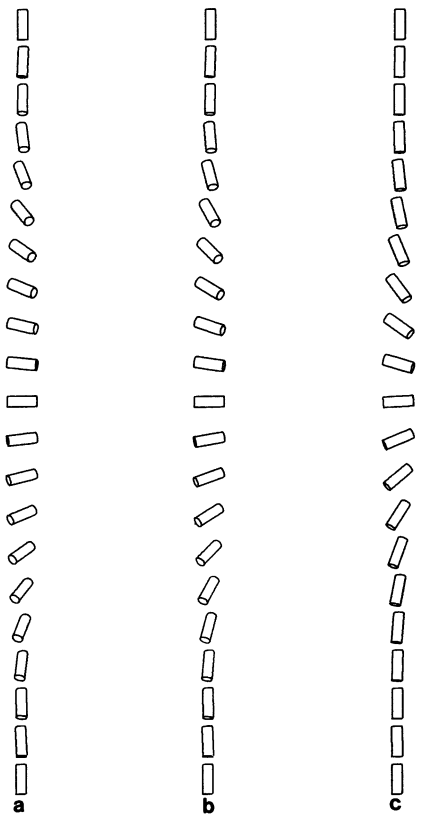

FIG. 3. — A possible molecular structure for a cholesteric in the 0-π configuration subject to homeotropic pinning conditions. In (*a*) there is no applied magnetic field and a partially formed cholesteric helix is seen. A moderate (*b*) and strong (*c*) magnetic field applied perpendicular to the top and bottom surfaces tightens up the turn-over region near the midplane but cannot drive the sample to the homeotropic configuration because of the surface pinning.

about the field direction whereas for figure 3*c* the field of view will vary in brightness as the sample is rotated.

We find that for a typical sample (wedge angle $\sim 1^{\circ}$) containing the finger-like region we are always confronted with a least one singular line which occurs at thicknesses about twice that at which the fingers nucleate from the homeotropic (which we call Z_c). This behaviour is found for a wide range of pitches (the pitch can be varied by changing the concentration, e.g., of cholesteryl oleate in MBBA) and as Z_c scales with pitch, the effect observed must be intimately connected with the cholesteric wavenumber $q(= 2\pi/$ pitch). For samples with larger wedge angles ($\sim 3^{\circ}$) we often see 3 or 4 lines running approximately perpendicular to the wedge gradient as shown in figure 4.

At the thinnest edge of the wedge (the bottom of figure 4) the molecules align homeotropically between the two glass plates and the sample between crossed polarizers is dark. At a critical thickness Z_c [1], the PC finger structure nucleates with the fingers parallel to the direction of the flow, which in this preparation was parallel to the direction of the thickness gradient (from top to bottom in figure 4). At a thickness determined by the pitch of the cholesteric, the finger structure rotates by 90° and the fingers are perpendicular to the previous flow direction. This rotation is related to the nature of the PC (related to the mean molecular orientation). This re-orientation of the fingers is continuous, there are no singular lines present. At a thickness determined by the pitch, the finger structure again rotates by 90°; however, this time a singular line separating the two structures can be seen. As one looks towards the thicker end of the sample, a small transition region consisting of spiralling fingers is observed leading to straight fingers perpendicular to the previous flow direction. These transitions take place continuously. A second singular line is then encountered and the finger structure is again generally more aligned with the flow direction, followed by a spiralling region and another linear region with the fingers perpendicular to the flow direction. A third singular line can be seen with difficulty near the top of figure 4. As the sample becomes thicker this pattern should reproduce itself many times, but the driving forces quickly become too weak to overcome randomizing effects due to impurities, poor surface preparation, and other disorienting factors. Across the singular lines the direction of translational invariance

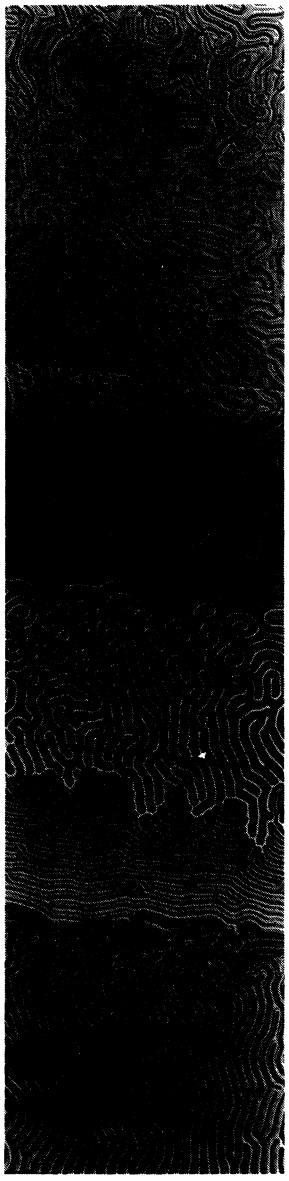

FIG. 4. — A 3 % solution of Ch—Ol in MBBA in which most of the random disclination lines have been eliminated (cleaned up) by manipulating the glass slides. The wedge angle is several degrees and the liquid is thinnest at the bottom. Three disclination lines and many different distinctive regions can be seen. The previous flow was from top to bottom. The periodicity is approximately 10 μ.

of the periodic cholesteric (PC) configuration changes by 90° and the connectedness between the surfaces changes from 0-0 to 0-π, as can be verified by a vertical magnetic field.

The nature of the straight fingers has been described previously [1]. The spiralling fingers are three dimensional and are beyond our computing capabilities. Experimentally it appears that these spiralling structures are the lowest energy, except near the critical thickness Z_c, and that they will dominate the rest of the structure if the sample is left undisturbed overnight. Calculations performed assuming cylindrical symmetry indicate that the inner two circular fingers are slightly lower in energy than fingers in a linear arrangement. This probably explains why the spiral structures with one or two revolutions dominate the pattern after a long undisturbed period.

We will show that the singular lines are the remnants of Grandjean lines, that they are produced during the shear flow processes when the structures are nucleating, and that they serve the same purpose as commonly accepted Grandjean lines, namely to relieve the strain energy associated with a cholesteric twist different from that of the equilibrium pitch in a wedge cell.

When the sample is sheared, the PC configuration is destroyed and the Translationally Invariant Cholesteric (TIC) configuration (no spatial derivatives in the plane of the sample) is produced. When the flow has ceased the PC configurations nucleate out of the TIC as shown in figure 5 and described previously [1], the direction of the fingers being largely determined by the nature of the parent TIC and the direction of the relaxing shear flow. In this paper, we will concentrate on the effects of flow on the structure and strain energies of the TIC configuration since these calculations contain the essential explanation for the production of the singular lines, and are much less consuming of computational time than a full treatment of the PC configuration.

a)

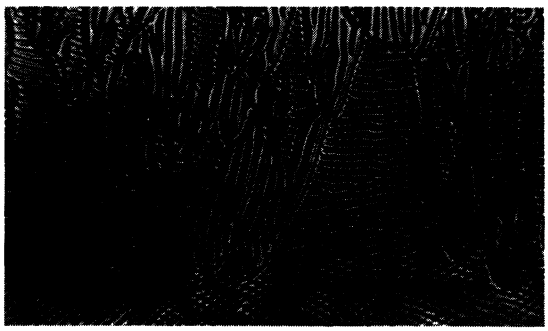

b)

FIG. 5. — As the flow of the liquid (from bottom to top) decreases the PC finger structure starts to nucleate out of the TIC as shown in (*a*). Many singular lines are present. A few seconds later (*b*) the PC structure is well established. Across the singular lines the finger structures are usually orthogonal. The cross-hatched pattern near the bottom of (*b*) is an intermediate structure and will disappear. It occurs in the region where the finger structure rotates by 90° without any singularities present.

2. **Energy and torque equations.** — For the TIC configuration all derivatives in the plane of the sample (x-y plane) are zero (neglecting here the small wedge angle), thus only derivatives along the perpendicular to the plane (the z-axis) appear.

With a director field given by the direction cosines

$$n = \hat{\mathbf{i}}\alpha + \hat{\mathbf{j}}\beta + \hat{\mathbf{k}}\gamma \tag{1}$$

the strain energy per unit area of sample is

$$E_a = \tfrac{1}{2} K \int \mathrm{d}z(\alpha_z^2 + \beta_z^2 + \gamma_z^2 + 2\, q(\alpha\beta_z - \beta\alpha_z) + q^2) \tag{2}$$

where K is an elastic constant, and the subscripts denote derivative. The treatment here is restricted to the simplified case with $K_{11} = K_{22} = K_{33} = K$. Minimizing this energy with respect to all variations of the director produces the coupled torque equations

$$\alpha_{zz} = \lambda\alpha + 2\, q\beta_z\,, \tag{3a}$$

$$\beta_{zz} = \lambda\beta - 2\, q\alpha_z\,, \tag{3b}$$

and

$$\gamma_{zz} = \lambda\gamma \tag{3c}$$

where the Lagrange multiplier $\lambda(z)$ is introduced to handle the unit vector constraint ($\hat{\mathbf{n}}.\hat{\mathbf{n}} = 1$). This has been described more fully in a previous paper [2] along with methods of solution on a computer.

When a flow is applied to the sample, further torques act upon the director field. These torques [3] are given by the molecular field

$$\mathbf{h}_{\text{flow}} = \gamma_1 \left(\frac{\mathrm{d}\hat{\mathbf{n}}}{\mathrm{d}t} - \boldsymbol{\omega} \times \hat{\mathbf{n}} \right) + \gamma_2\, \hat{\mathbf{n}}.\mathbf{A} \tag{4}$$

where

$$\boldsymbol{\omega} = \tfrac{1}{2} \nabla \times \mathbf{v} \tag{5a}$$

and

$$A_{\alpha\beta} = \tfrac{1}{2}(\partial_\alpha v_\beta + \partial_\beta v_\alpha)\,. \tag{5b}$$

In equations (4) and (5), $\mathbf{v}$ is the velocity field,

$$\gamma_1 = \alpha_3 - \alpha_2 \tag{6a}$$

and

$$\gamma_2 = \alpha_3 + \alpha_2 \tag{6b}$$

where α_2 and α_3 are two of the Leslie coefficients [3]. (We regret the possible confusion between the direction cosines α and γ and the coefficients α_2, α_3, γ_1, and γ_2, they are unrelated but are conventionally accepted.)

For time independent flow fields in translationally invariant steady state samples

$$\frac{\mathrm{d}\hat{\mathbf{n}}}{\mathrm{d}t} = \frac{\partial\hat{\mathbf{n}}}{\partial t} + (\mathbf{v}.\nabla)\,\hat{\mathbf{n}} = 0\,. \tag{7}$$

With a flow along the y-direction the flow molecular field becomes

$$\mathbf{h}_{\text{flow}} = \frac{\mathrm{d}v}{\mathrm{d}z}[\hat{\mathbf{j}}\gamma\alpha_2 + \hat{\mathbf{k}}\beta\alpha_3]\,. \tag{8}$$

Adding this term to equation (3) results in the equations

$$\alpha_{zz} = \lambda\alpha + 2\, q\beta_z\,, \tag{9a}$$

$$\beta_{zz} = \lambda\beta - 2\, q\alpha_z - \frac{\alpha_2}{K}\frac{\mathrm{d}v}{\mathrm{d}z}\gamma\,, \tag{9b}$$

and

$$\gamma_{zz} = \lambda\gamma - \frac{\alpha_3}{K}\frac{\mathrm{d}v}{\mathrm{d}z}\beta \tag{9c}$$

which must be satisfied for a static equilibrium in the presence of a constant shear flow. Experimentally for MBBA at room temperature $\alpha_3/\alpha_2 \sim 0.02$ [3], thus the term added to the β equation (eq. (9b)) is the most important but the α_3 term in equation (9c) becomes significant when $\gamma \sim 0$.

The torque on the molecular structure is given by

$$\boldsymbol{\tau} = \hat{\mathbf{h}} \times \hat{\mathbf{n}}$$

$$= \frac{\mathrm{d}v}{\mathrm{d}z}[\hat{\mathbf{i}}(\alpha_2\,\gamma^2 - \alpha_3\,\beta^2) + \hat{\mathbf{j}}\alpha_3\,\alpha\beta - \hat{\mathbf{k}}\alpha_2\,\alpha\gamma]\,, \tag{10}$$

Again since $\alpha_2 \gg \alpha_3$ the most interesting torques are those about the x- and z-axes. Both these terms are proportional to γ and thus disappear when γ is zero, i.e. when the director lies in the x-y plane. The importance of this point will be emphasized in the next section where the explanation for the existence of the Grandjean-like lines is outlined.

3. **Ideas and calculations.** — The flow is treated in an approximate manner. When the sample fluid is flowing between two parallel glass plates, to a first approximation, the direction of the flow is parallel to the plates, along the y-direction. In practice, there will be deviations from this idealized behaviour due to the anisotropy in the viscosity. This added feature was exploited by Guyon and Pieranski in their production of vortice cells [4]. For low speeds, of the order of microns/second, these additional effects can be neglected. The velocity points in the y-direction and varies from 0 at the surfaces to some $v_{\max}$ in the middle plane. For a parabolic velocity profile, chosen for simplicity,

$$\mathbf{v}(z) = \hat{\mathbf{j}} v_{\max}\left[1 - \left(\frac{2\,z}{Z}\right)^2\right], \tag{11a}$$

where z is measured from the mid plane and the plate separation is Z. This produces a linear velocity gradient

$$\frac{\mathrm{d}\mathbf{v}}{\mathrm{d}z} = -\hat{\mathbf{j}} v_{\max}\, 8\, z/Z^2$$

$$= \hat{\mathbf{j}} F z \tag{11b}$$

where F is the parameter which determines the strength of the shear flow.

The effect of this flow on the molecular arrangement for samples with homeotropic constraints ($\gamma = \pm 1$) at the surfaces ($z = \pm Z/2$) is first discussed qualitatively and then in terms of the results of the computer calculations.

The main effect can be seen by initially considering a nematic liquid ($q = 0$). Starting from the homeotropic configuration (Fig. 6*a*), we first look near each surface where the effect of the shear torque (Eq. (10)) will be to tip the director over as shown in figure 6*b* due to the flow gradient. For sufficient gradient, the director will lie in the y direction near both surfaces. If the director is taken as lying in the $+ z$ direction at each surface, then the director near the two surfaces will point in opposite directions. If the directors are tilted other than as shown, the configuration will be unstable and when released will rotate to the proper configuration.

Next it is necessary to connect these two regions lying in opposite directions. If we constrain the molecules to the plane of the paper (the y-z plane) then two configurations suggest themselves. In the first of these, the director continues to be close to the y-direction as shown in figure 6*c*. There are negligible torques on these molecules since the z-derivatives approach zero (no strain energy) and the molecules lie in the direction of flow (i.e. $\gamma = 0$) and thus the main torque terms are zero. The smaller terms due to α_3 are still present but they are small in magnitude. Note that in going from figure 6*b* to figure 6*c*, it has been necessary to relabel the director in the bottom layer and as a consequence the boundary conditions are 0-π rather than 0-0.

We thus consider the sample as having two surface layers, each of thickness ε in which the shear flow is important and a central layer of thickness $Z - 2\varepsilon$ in which the shear flow to a first approximation can be neglected. For sufficiently large shears, it can be shown that ε varies inversely as the square root of the shear flow near the surface.

In the second planar configuration, figure 6*d*, the director rotates through $\gamma = 1$ in the central plane. This configuration has splay and bend energy in the central region while the first had none. As long as the molecular configurations near the surfaces for the two cases are similar, the second configuration would be of higher strain energy than the first.

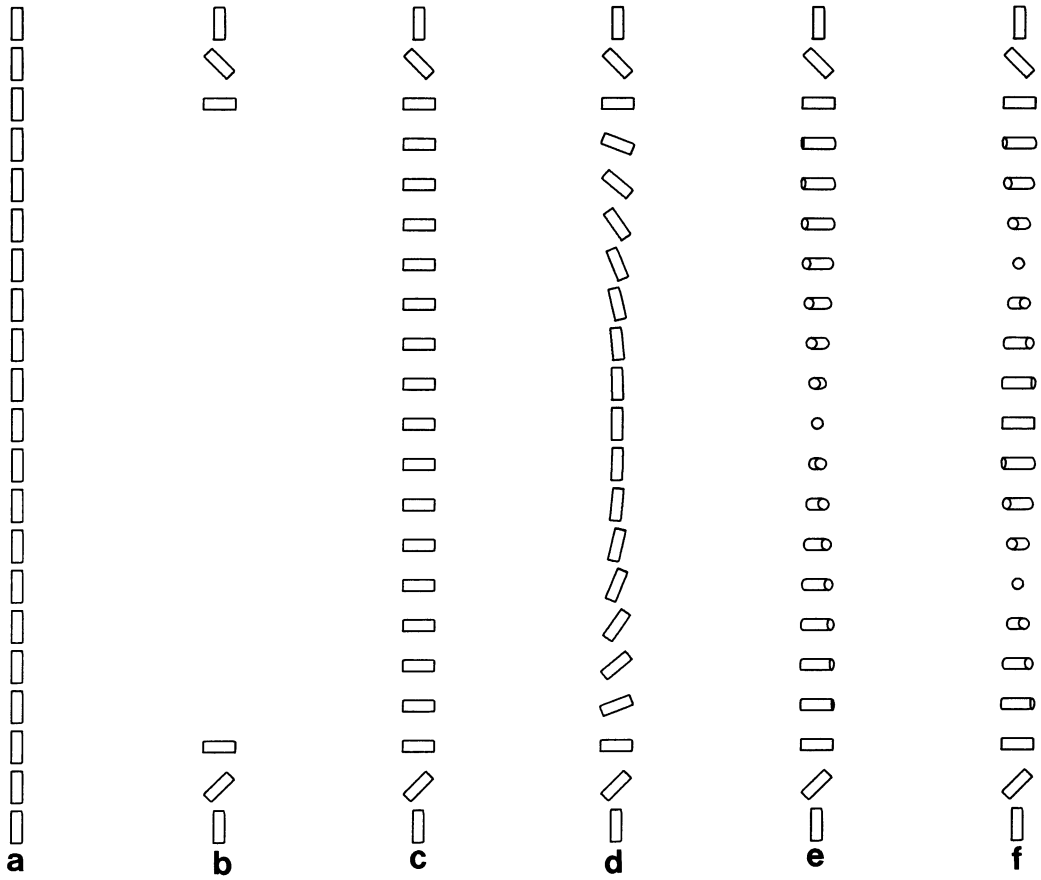

FIG. 6. — The director field for a nematic liquid between glass plates treated to give a homeotropic surface alignment. The homeotropic alignment is shown in (*a*). In a strong flow to the right the director field near each surface rotates into the flow (*b*). Two possible planar configurations to connect the surface director fields suggest themselves. One is a 0-π structure (*c*) while the other (*d*) is a 0-0 configuration. When the molecular field is free to rotate out of the page, many other configurations are possible. With a 180° rotation of the director about the surface normal (*e*) a 0-0 structure is produced while with a 360° rotation (*f*) a 0-π structure is formed.

The significant point is that the second configuration (Fig. 6*d*) can be achieved continuously from the homeotropic. This is a 0-0 type configuration. The first, figure 6*c*, is a 0-π type and can be obtained from the homeotropic only through some discontinuity, such as nucleating a bulk line or breaking the surface pinning. Once it has been nucleated it then cannot disappear without the nucleation of a further line, and it will remain 0-π as the flow is decreased.

Even though the 0-0 type has higher energy than the 0-π type, it is not necessarily unstable with respect to it. It would be necessary to consider in detail the nucleation of the lines or loops responsible for the transition.

Other possible configurations can be realized by letting the director rotate out of the page as shown in figures 6*e* and 6*f* and other such constructions. The configuration of figure 6*e* (a 0-0 type) has twist energy in the central region making it of higher energy than the configuration of figure 6*c* but not necessarily unstable with respect to it, or even with respect to the figure 6*d* configuration. The configuration of figure 6*f* (a 0-π type) has still higher twist energy and would likely be unstable with respect to the configuration of figure 6*c*.

We therefore have the interesting case where the 0-0 configuration is the lowest energy at low shear (including zero shear for which the homeotropic configuration has zero energy) while the 0-π configuration (Fig. 6*c*) is lowest in energy for sufficiently high shear rates. Thus as the flow increases in a parallel plate sample, we might expect to see a discontinuity occur in the director field and to find that 0-π regions have nucleated.

The results of computer calculations are shown in figure 7 for several thicknesses. The energy density refers to the elastic strain energy. The dissipative flow is non-conservative. What really matters are the torques, the relative stability of two regions in contact will depend upon the specifics of the boundary between them, and not just upon the differences of elastic energy. Nevertheless, the elastic energies are indicative of how lines or loops separating regions might move. At a given thickness the configurations near the surfaces are almost identical, especially for the larger flow rates. The line $N = 0$ corresponds to no initial twist built into the starting solution, i.e. it corresponds to figure 6*c* and is a 0-π configuration.

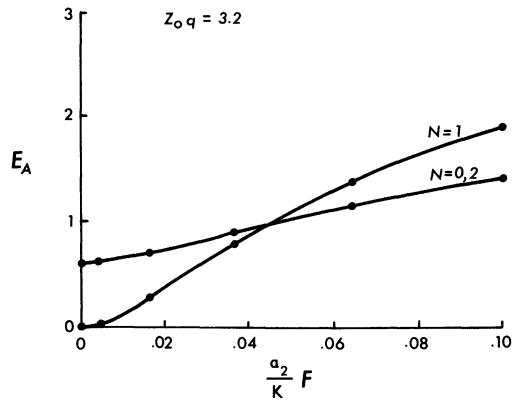

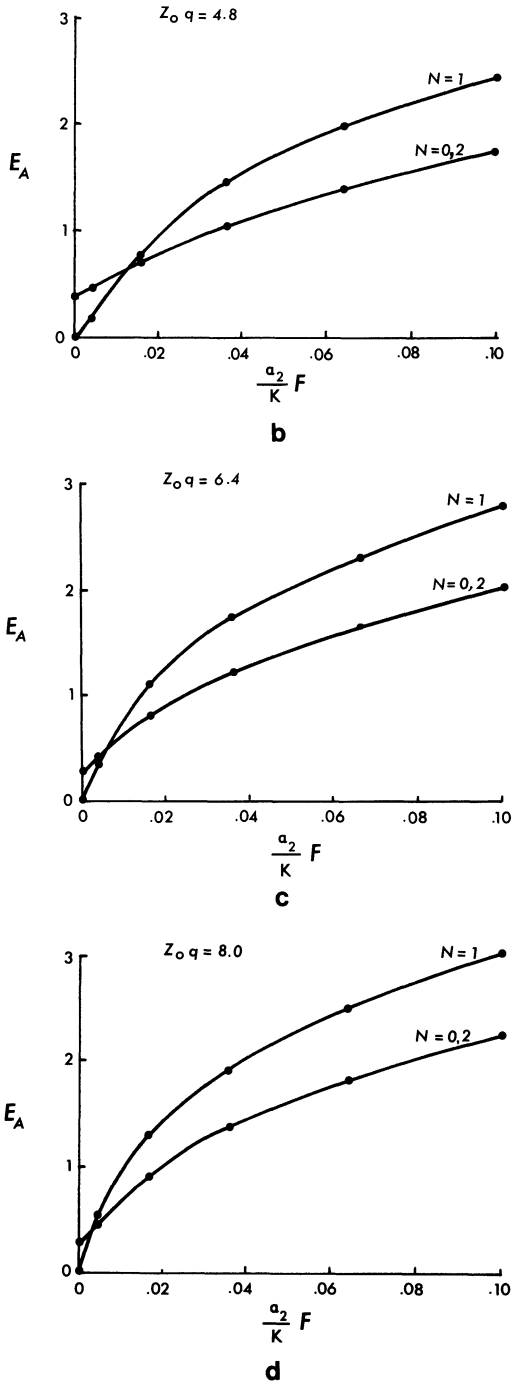

FIG. 7. — Nematic liquid crystal under shear flow conditions showing the elastic energy per unit area (in units of 2.5 Kq) as a function of the flow parameter F (in units of q^2) for thicknesses $Zq = 3.2$ (*a*), $= 4.8$ (*b*), $= 6.4$ (*c*) and $= 8.0$ (*d*). The calculations were started at high shear flow with an imposed number of half (180°) rotations N and allowed to relax as the flow constant was reduced. When a structure with a given N immediately collapses it is shown on the same curve as the structure to which it changes. At high flow rates the $N = 0$ structure is lowest in energy while for low flow rates the $N = 1$ structure has the lowest strain energy.

$N = 1$ corresponds to a starting solution with one π rotation of the director field and corresponds to figure 6*e*. This solution is unstable and collapses to the configuration of figure 6*d*. It is a 0-0 type of configuration. Higher order starting twists have been tried. Some are stable at very high flow rates for thick samples but they all collapse into the two basic configurations of figures 6*c* and 6*d* as the flow is reduced, at least in the one elastic constant approximation used here. [Using the true values for the splay, twist and bend constants might change these results since for MBBA the twist constant is less than the splay and bend constants. Since this is not the main effect we are after, this line of enquiry has not been pursued.]

Figure 7 shows the expected results for a nematic under flow. For low shear rates, the 0-0 configuration is lower energy than the 0-π configuration. As the shear flow is increased there is a critical rate, depending on the thickness, at which the energy for the 0-π configuration becomes lower than that for the 0-0 configuration. This critical rate decreases as the thickness increases. When the energy difference becomes larger than the nucleation barrier separating these two configurations, the 0-π should form.

It is difficult to make quantitative comparisons between different thicknesses. We have chosen in our graphical analysis to show the elastic strain energy as a function of the shear parameter F. This is not entirely fair since a thick sample will experience a larger shear than a thinner one for the same F (Eq. (11)). Other methods of comparing the flow effect for different thicknesses suggest themselves. One could compare different thicknesses with the same shearing force at the surfaces, the energy would then be related to F/Z. If one wanted to compare samples with the same maximum velocity, the energy should be determined as a function of F/Z^2. Finally, one could compare different thicknesses with the same mass flux of liquid which is how the experiment is done using a wedge. This requires that the energy be calculated as a function of F/Z^3. The computer calculations were done with the idea of a parallel plate geometry in which the shear parameter could be controlled by applying the appropriate pressure gradient to the liquid, thus we have shown the dependence of the energy upon the shear parameter and have made no attempt to directly intercompare the results for different thicknesses. A certain amount of scaling can be seen for the $N = 1$ nematic structures where the energy is roughly proportional to $\sqrt{FZ}$, but this disappears when we concentrate on the cholesteric structures which are the focus of this paper.

When the nematic material is replaced by a cholesteric, still subject to homeotropic pinning at the surfaces, the same major effects are observed on the computer. However, the energies are different. Since the cholesteric likes to twist, the energy for the configuration of figure 6*e* can now become lower than that for the configuration described in figure 6*c*. This depends on how the rate of rotation of the director field with z compares with the equilibrium wavenumber q. Thinking in terms of polar coordinates θ (measured with respect to z) and φ (measured with respect to x) ($\alpha = \sin\theta\cos\varphi$, $\beta = \sin\theta\sin\varphi$ and $\gamma = \cos\theta$), the energy density in the central region, in which $\theta \sim 90°$, becomes

$$f = \tfrac{1}{2} K(\varphi_z + q)^2 . \qquad (12)$$

For strong shear flows $\left(\left| \frac{\alpha_2}{K} \frac{\mathrm{d}v}{\mathrm{d}z} \right| \gg |q| \right)$ we can take $\beta = \cos\varphi = \pm 1$ near the surfaces, pinned there by the shear flow. Under these conditions, the average value of φ_z through the bulk will be equal to $-\frac{N\pi}{Z - 2\varepsilon}$ where N is an integer which determines how many half rotations the director makes in going through the central region. Neglecting ε (for large shear flow $\varepsilon \ll Z$), we see that $\left(\frac{N\pi}{Z} + q\right)^2$ is a minimum for different values of N as Z increases. The best value of N can be determined by picking the integer closest to $-Zq/\pi$. Thus, the integer N increases in a step-wise fashion with Z as shown in figure 8 for a greatly exagerated wedge angle. Between these different configurations there must be lines of discontinuity analogous to Grandjean lines and arising for the same reason, namely to reduce the twist strain energy. Also, the configurations with N even are 0-π types of solution, as can be seen by following the director, while for N odd the structures are 0-0 solutions. The

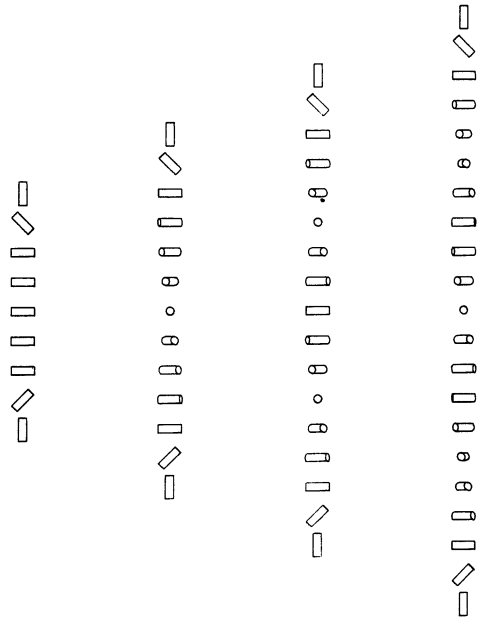

FIG. 8. — The cholesteric configuration of lowest strain energy (with homeotropic surface pinning) in a strong flow to the right changes in a stepwise fashion as the thickness of the liquid increases. From left to right $N = 0$, 1, 2 and 3. The structures with N even are 0-π while for N odd the structures are 0-0. Between successive structures there must be singular lines.

connectedness between the surfaces is maintained after the flow is stopped, since, once the Grandjean-like pinning is relaxed, the structure can rotate to that of minimum energy, which we have shown previously [1]. corresponds to $\varphi_z = -q$ because of the homeotropic pinning at the surfaces. Thus, even after the flow has ceased, the singular lines, which once were Grandjean lines, remain, now as disclination lines separating the 0-0 and 0-π regions. In zero flow the 0-π regions are higher energy than the 0-0 regions (in the one-constant approximation) but cannot relax to them because of the nucleation energy involved (the energy difference between the 0-0

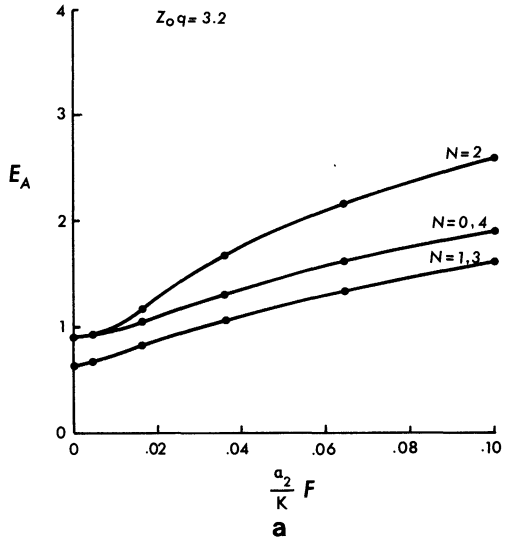

FIG. 9. — Cholesteric liquid crystal under shear flow conditions showing the elastic strain energy (in units of 2.5 Kq) as a function of the flow parameter (in units of q^2) for thickness $Zq = 3.2$. For $Zq < 6.4$ the $N = 1$ structure is lowest in energy; for $6.4 \lesssim Zq < 9.6$ the $N = 2$ structure is lowest; for $Zq \sim 9.6$, the $N = 3$ structure has the lowest energy. Many of the configurations of higher energy are also possible as shown in these graphs. The flow behaves to some extent like weak planar pinning of the Chatelaine type which can be overcome when the flow is slow enough.

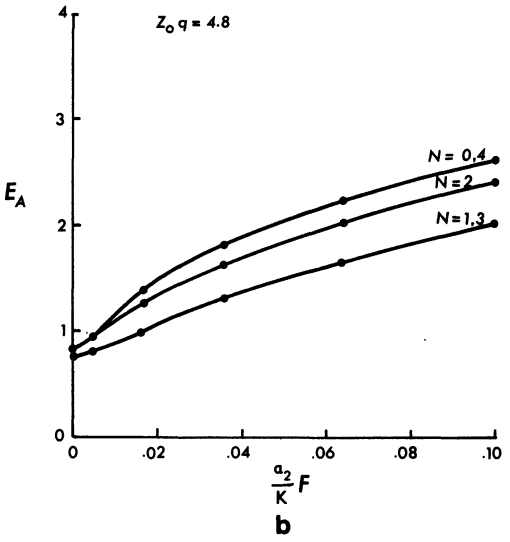

FIG. 9*b*. — $Zq = 4.8$.

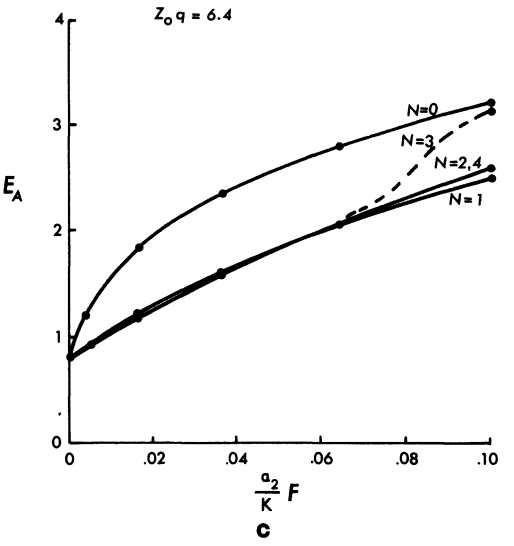

FIG. 9*c*. — $Zq = 6.4$.

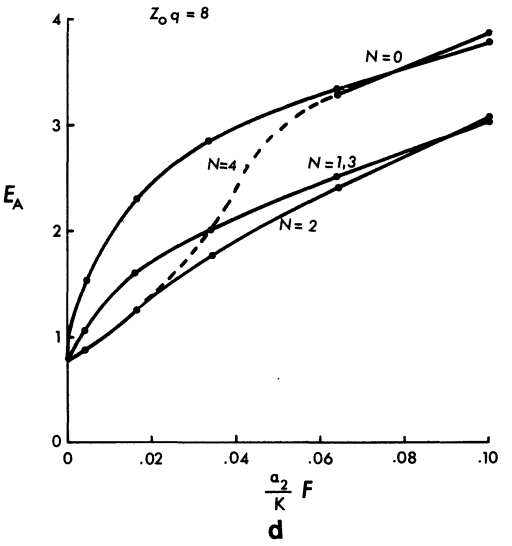

FIG. 9*d*. — $Zq = 8.0$.

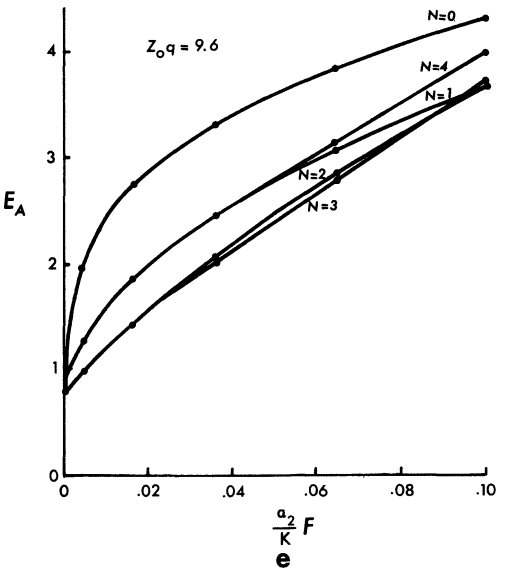

FIG. 9*e*. — $Zq = 9.6$.

and 0-π in zero flow can be much less than the difference in strain energy between an N and an $N + 1$ configuration in large flow).

The strain energy for several thicknesses and flow rates for different starting values of N as calculated by computer in the one constant approximation are shown in figure 9. For $Zq = 3.2$, figure 9*a*, the configuration with $N = 1$ is of lowest energy for all flow rates. This is a 0-0 type of configuration. The configuration with $N = 0$, a 0-π structure, is of higher energy. An initial configuration with $N = 3$ immediately collapses into the $N = 1$ configuration for the shear rates used. It is possible to get an $N = 2$ configuration, stabilized by the shear flow but which finally collapses to the lower energy $N = 0$ structure when the flow is sufficiently lowered. A starting structure with $N = 4$ has so much energy that it immediately collapses to the $N = 0$ structure, by passing through the intermediate energy $N = 2$.

For $Zq = 4.8$ (Fig. 9*b*), the $N = 1$, a 0-0 structure, is still the lowest energy but now the $N = 2$, a 0-π structure is next lowest in energy, the $N = 0$ having become much more costly.

For $Zq = 6.4$ (Fig. 9*c*), the $N = 1$ structure is lowest in energy at high flow rates but at intermediate shear flows the $N = 2$ structure, a 0-π configuration, is lowest in energy. Also seen is a distinct $N = 3$ structure at high flows which collapses to the $N = 1$ structure for intermediate and low shear flow rates.

For $Zq = 8.0$ (Fig. 9*d*), the $N = 2$, a 0-π structure, is the lowest energy for the intermediate shear flow rates examined. At this thickness we have an example in which the 0-π structure is considerably lower in energy than the 0-0 structure, except for a small inversion at zero and at large flows.

For $Zq = 9.6$ (Fig. 9*e*), the $N = 3$, a 0-0 structure, is lowest energy for intermediate flow rates but $N = 2$ does become slightly lower at the highest shear flow examined.

These variations in energy for the different structures arise largely due to the difference in the rate of twist compared to the equilibrium twist q. The variation of φ with z is shown in figure 10 for $Zq = 8$ with $N = 1$ and 2 for a large shear flow rate. Near

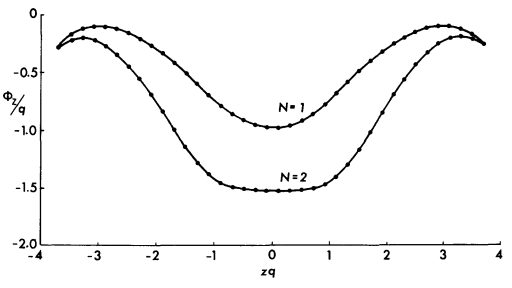

FIG. 10. — The variation of the rate of rotation of the director field in the basal plane with position between the glass plates for a sample thickness $Zq = 8$. The $N = 2$ structure has a mean rate of rotation φ_z closer to the unconstrained cholesteric ($\varphi_z = -q$) than the $N = 1$ structure and therefore has lower twist (and total strain) energy.

the surfaces φ_z is small. This is due to the soft homogeneous pinning caused by the large shear flow. Towards the central region φ_z/q increases to about -1 for $N = 1$ and to about -1.5 for $N = 2$. However, the average value of φ_z/q for $N = 1$ is about -0.5 and for $N = 2$ about -1. The $N = 2$ configuration has an average value of twist closer to the equilibrium value ($\varphi_z/q = -1$) than the $N = 1$ solution and will have a lower twist energy. Since the splay and bend energies (found mostly in the surface transition layer) for the two configurations are similar, the $N = 2$ configuration will have a lower total energy than the $N = 1$ case.

Thus as the thickness increases, we expect the 0-0 and 0-π solutions to alternate being of lowest energy. The first important crossover (between $N = 1$ and $N = 2$) occurs for $Zq \sim 6.4$ or about $2\,Z_c$ ($Z_c\,q = 3.2$ from [1]) which agrees with our experimental observations. The crossover between $N = 0$ and $N = 1$ for high shear flows occurs at about the critical thickness, Z_c, at which the TIC nucleates from the homeotropic. This line is sometimes seen if the flow rate becomes large enough in these thinner regions. The crossover between $N = 2$ and $N = 3$ should occur at about $Zq = 9.6$ ($3\,Z_c$), again in agreement with our observations. The singular lines should be approximately equally spaced in the wedge plate construction. This can be observed in figure 4.

In actual samples the TIC configuration with no flow is itself unstable with respect to the PC configuration and breaks up into these finger regions as described previously [1]. Both 0-0 and 0-π type PC configurations are possible. The type and orientation of these fingers is determined by the parent TIC configuration. For even-N TIC configurations, the central director points in the direction of the flow while for odd-N the central director points perpendicular to the flow direction. When the PC configuration nucleates from the TIC it is not unreasonable to expect that the orientation of the fingers for even-N would be perpendicular to that for odd-N, yet it is difficult to give a completely rigorous sequence for the nucleation processes. This would require a determination of the periodicity of minimum energy as a function of the flow rate for the two structure types (0-0 and 0-π), for the relative orientation of the flow with respect to the finger structure and for the various orders of twisting (N). Similar calculations have been done for the effects of magnetic and electric fields on the PC structure. The calculations, reported elsewhere [2], and the similarities between shear flow and magnetic and electric fields in aligning the director produce a qualitative understanding of the PC structure in a shear flow. The observed destruction of the PC in favour of the TIC as the shear flow is increased and the reverse as the shear flow is decreased is entirely within expectation and no new important information would be obtained through further calculation. For quantitative comparison with experiment

the full three constant equations ($K_{11} \neq K_{22} \neq K_{33}$) must be used in addition to calculating the true viscous flow. This is a much more difficult problem.

4. **Conclusion.** — A cholesteric liquid crystal constrained between homeotropic-inducing glass plates show many interesting features. In this paper attention has been focussed on the singular lines that exist separating various regions of the sample. These have been shown to be related to Grandjean lines, produced while the sample is being subjected to a shearing flow. These lines separate regions of the sample in which the orientation of the director field between the glass slides can be derived continuously from the homeotropic (0-0) or cannot be thus derivied without some discontinuity (0-π). In a *cleaned up* wedge sample, these singular lines should be approximately parallel to the constant thickness contours and should be roughly equally spaced by a distance related to the wedge angle and the equilibrium wavenumber. After the flow has ceased these singular lines can either stay in the bulk of the sample or migrate to the constraining surfaces if the surface pinning is not infinitely strong. Both types of singular lines, which can be differentiated by their mobility in a flow, are observed.

References

[1] PRESS, M. J. and ARROTT, A. S., *J. Physique* **37** (1976) 387.
[2] PRESS, M. J. and ARROTT, A. S., *Mol. Cryst. Liq. Cryst.* **37** (1976) 81.
[3] DE GENNES, P. G., *The Physics of Liquid Crystals* (Clarendon Press) 1974 Ch. 5.
[4] GUYON, E. and PIERANSKI, P., *J. Physique Colloq.* **36** (1975) C1-203.